NONLINEAR CONTROL THEORY FOR A CLASS OF STRUCTURAL NONLINEARITIES IN A PROTOTYPICAL WING SECTION

Jeonghwan Ko*, Andrew J. Kurdila† and Thomas W. Strganac‡
Department of Aerospace Engineering
Texas A&M University
College Station, TX 77843-3141

Abstract

With the increase in popularity of active materials for control actuation, renewed interest is evident in the derivation of control methodologies for aeroelastic systems. It has been known for some time that prototypical aeroelastic wing sections can exhibit a broad class of pathological response regimes when the system includes certain types of nonlinearities. In this paper, we investigate nonlinear control laws for aeroelastic systems that include polynomial structural nonlinearities, and study the closed loop stability of the system. It is shown that locally asymptotically stable (nonlinear) feedback controllers can be derived for the aeroelastic system using partial feedback linearization techniques. In this case, the stability results are necessarily local in nature and are derived by considering stability of the associated zero dynamics subsystem. It is also demonstrated that globally stable (nonlinear) adaptive control methods can be derived for a class of aeroelastic systems under consideration. Numerical simulations are used to provide empirical validation of some of the results in this paper.

1 Introduction

The authors examine active control of aeroelastic response and, in particular, address appropriate control strategies for nonlinear aeroelastic systems. Aeroelasticity is the interaction of structural, inertial and aerodynamic forces. Flutter is an oscillatory aeroelastic instability characterized by the loss of system damping due to the presence of unsteady aerodynamic loads (see Fung[6]) Theodorsen[24] developed the classical unsteady aerodynamic theory which accounts for the aerodynamic (lag) damping at different flow conditions and frequencies. Theodorsen and Garrick[25] predict flutter velocities and frequencies, and compare these predictions of flutter with experimental results. Wagner and Jones[27] develop approximations of Theodorsen's function which are appropriate to simulate wing motion and predict aeroelastic response in unsteadyaerodynamic flow.

Using the developments by Wagner and Jones, several researchers have attempted to further understand the control of unsteady motion of an airfoil. Lyons et al.[17] used a method of converting the Jones approximation into the Laplace domain and augmenting the states of the system to account for the lag terms in the aerodynamics. This approach structured the equations of motion for control law development. Vepa[26] developed a Padé approximation technique to describe both Wagner's function and Theodorsen's function in the frequency domain. Edwards et al.[5] compared the methods of Lyons and Vepa. Furthermore, Edwards examined these developments by dividing the circulatory terms of the lift into "rational" and "nonrational" portions since the "nonrational" part could not be written as a ratio of polynomials. Edwards' approach reduced the number of augmented states previously required to model the unsteady aerodynamics. These methods are developed for arbitrary, but small, motion of a wing.

Many strategies have been examined to con-

*Postdoctoral Research Associate, Member AIAA.
†Associate Professor, Member AIAA.
‡Associate Professor, Associate Fellow AIAA.

trol unacceptable wing response or suppress flutter. Lyons et al.[17] investigated full-state feedback with a Kalman estimator for the purpose of flutter suppression. The theoretical model was relatively simple and required only eight states. Mukhopadhyay et al.[18] and Gangsaas et al.[7] created 20th and 50th order models, respectively. They developed methods to reduce these higher-order systems to show the practicality of these control strategies. These control systems implemented estimators to describe unmeasured states and used state feedback as the control method. Karpel[12] compared the aerodynamic descriptions of Lyons, et al., Vepa, and Edwards, et al. to develop partial-state feedback controllers. Karpel used pole placement techniques to develop the control laws for flutter suppression and gust alleviation.

Horikawa and Dowell[10] performed flutter analysis with control, employing proportional gain feedback methods developed from root locus plots. They used a quasi-steady aerodynamic model coupled with a two degree-of-freedom structural model to develop several types of feedback. The development directly feeds one of four variables to the control surface through a proportional gain. Heeg[9] investigated flutter suppression by control with piezoelectric actuators, and increased the flutter velocity by 20%. The work involved a small wing model mounted on spring tines to simulate the bending and torsion modes. Four actuators were mounted to control the bending mode. Heeg's analysis employs a classic approach for control, by using root locus plots to derive proportional gain feedback control laws.

Lin[16] and Lazarus[13, 14] analyzed a typical section model. The study included control of the bending and torsion modes by piezoelectric actuators mounted on the wing and additional control with leading and trailing edge flaps. This structure and control scheme was designed for wind tunnel disturbance rejection, gust alleviation, and flutter suppression. They showed that direct control through piezoelectrics was possible. Their design strategy used full-state feedback with an estimator. Lazarus performed a more complete experimental analysis to validate the results of the typical section model.

These researchers have shown that linear theory can be applicable for control of aeroelastic systems. Unfortunately, as aircraft performance increases, so does the needs for more sophisticated aeroelastic models. Aeroelastic systems typically contain nonlinearities which are either neglected or simplified to a linear form for analysis. Nonlinearities which occur in aeroelastic systems include control saturation, free play, hysteresis, piece-wise linear, and continuous nonlinearities. Control saturation occurs when an increasing input into a system will no longer increase the output of the system. This nonlinearity occurs in most motor controllers when their operational limits are exceeded. Free play is seen in control surface linkages or hinges in which the surface will not move until the magnitude of the input exceeds a certain value. Hysteresis occurs in systems in which friction affects linkage dynamics or in which rivet connections slip on a wing. A nonlinear stiffness may be observed in the large bending of wings and rotor blades, or in control actuators that become increasingly harder to deflect as they are moved further from the neutral position. Many researchers have examined the nonlinearities inherent in structural models.

Woolston et al.[29] investigated nonlinearities in structural stiffness and control surface linkages. They created a model with free play, hysteresis, cubic-hardening and cubic-softening nonlinearities in the torsional mode. For general wing motion, they observed that the flutter velocity lowered as the initial disturbance grew and that the stability of the system was highly dependent on the magnitude of the initial condition. A cubic-softening spring stiffness lowered the flutter velocity. They also noted that cubic hardening caused limit cycle oscillations rather than flutter at velocities above the open loop flutter velocity.

Breitbach[2] shows that a poor agreement between theory and experiment in flutter is most likely due to nonlinear structural stiffness in models. He also presented a detailed examination of many types of nonlinearities that may affect aeroelastic systems. Tang and Dowell[23] introduced a free play nonlinearity in the torsional stiffness and examined the nonlinear aeroelastic response. For various initial conditions, they created maps of the system response to describe locations of periodic limit cycles, chaotic motion, and divergent motion. They concluded that limit cycle motion is dependent upon free stream velocity, initial pitch condition, magnitude of the free play nonlinearity and initial conditions.

Lee and LeBlanc[15] performed analysis of a nonlinear wing model using a time-marching scheme that simulated aeroelastic response. Models of softening and hardening cubic springs were examined by varying the mass ratio, increasing the distance between the elastic axis and the center of mass, and by varying the ratio of the plunge frequency to pitch frequency. For the softening spring case, unstable motion was encountered below the linear flutter speed for nearly every parameter; increasing the nonlinearity and increasing the mass ratio tended to make the system more unstable at lower velocities. For the

hardening spring case, limit cycle oscillations were always present instead of divergent flutter. Varying the parameters of the hardening spring case affected the amplitudes of the limit cycles.

These researchers have developed models for exploring nonlinear aeroelasticity and have also attempted to describe the motion with time marching solutions and describing function analysis. However, efforts to examine nonlinear aeroelasticity and active control strategies are limited. O'Neil, et al.[20, 21, 22] examines nonlinear aeroelastic response via a unique experimental apparatus which permits a prescribed linear or nonlinear structural stiffness. With nonlinear structural stiffness, the model exhibits limit cycle oscillations. Various full-state feedback control laws have been examined with the aeroelastic model with a control surface (see Block and Strganac[1]). An unsteady aerodynamic model is developed with an approximation to Theodorsen's function, and an observer, based upon the Kalman estimator, is used to estimate the augmented state system. Tests of the linear structural model and nonlinearities are examined while the performance of the control is verified for numerous flow conditions using the linear controller. In many flow regimes, the linear control design was highly effective. Roughly speaking, control of the nonlinear system during limit cycle oscillations was ineffective, unpredictable or poorly understood.

The premise of this paper is simple. While several authors have investigated the effectiveness of linear and adaptive control methodologies for aeroelastic systems, our own experimental investigations have provided empirical evidence that linear control methods may not be reliable when nonlinear effects predominate[1]. Typically, even less can be said about the closed loop stability of adaptive control methods. Thus, we seek to derive nonlinear control methodologies that make as much use of the knowledge of the nonlinearities as possible. In all of our analyses, a primary goal is to make definitive statements regarding the closed loop stability of the system. Our strategy has been to simplify the model and incorporate the essential and well-understood structural nonlinearities. It is to engage in understatement to say that the prototypical, aeroelastic system is subject to a wide class of nonlinearities. As will be noted, dead-zone, hysteretic, and polynomial nonlinearities in the structural system have been investigated. However, in comparison to the nonlinearities and uncertainties in the aerodynamic component of the dynamical system, the structural nonlinearities are well-characterized. To derive a controller that accounts for some of the nonlinearities in the system, we retain the nonlinear torsional stiffness terms. We feel that this dynamical system is the simplest possible model that remains a faithful representation of the physics we seek to address. If we neglect the structurally nonlinear terms, we do not observe limit cycle oscillations in our model near the critical velocity. Certainly, we can add additional nonlinear terms, particularly those that model aerodynamic effects, but the structurally nonlinear terms constitute the bare minimum required to represent limit cycle oscillations at low speeds.

The remainder of this paper discusses two control designs based on partial feedback linearization techniques. In the first case, we derive a nonlinear controller that guarantees the exponential stability of the "pitch dynamics subsystem." However, because the system is not fully feedback linearizable, decreasing pitch oscillations inject energy into the associated, remaining reduced degrees of freedom. Still, local asymptotic stability for the closed loop system can be established by considering the zero dynamics of the system. The local asymptotic closed loop stability of this "pitch primary" control depends parametrically on the flow velocity and elastic axis location. A similar control methodology is derived in the second part of the paper for the "plunge dynamics subsystem." Finally, this paper closes by showing that for a very simple, but structurally nonlinear, aeroelastic model with two control surfaces, the dynamical system is exactly feedback linearizable and global stability results can be derived.

2 Equations of Motion

In this paper, we consider the problem of flutter suppression for the prototypical aeroelastic wing sections as shown in Figure 1. This type of model has been traditional for the experimental and theoretical analyses of two dimensional aeroelastic behavior. The unique feature of the model considered herein is that the location of the elastic axis can be changed and various types of nonlinearities can be incorporated in the nonlinear stiffness for the pitch axis motion. Obviously, the two parameters – elastic axis location and free stream velocity – play critical roles in system stability. This fact is well-appreciated for the open loop system. A significant portion of this paper will study their importance in some closed loop control systems. As shown in [20, 21, 22], the governing equations of motion for the aeroelastic model

are derived to be

$$\begin{bmatrix} m & mx_\alpha b \\ mx_\alpha b & I_\alpha \end{bmatrix} \begin{Bmatrix} \ddot{h} \\ \ddot{\alpha} \end{Bmatrix} + \begin{bmatrix} c_h & 0 \\ 0 & c_\alpha \end{bmatrix} \begin{Bmatrix} \dot{h} \\ \dot{\alpha} \end{Bmatrix} + \begin{bmatrix} k_h & 0 \\ 0 & k_\alpha(\alpha) \end{bmatrix} \begin{Bmatrix} h \\ \alpha \end{Bmatrix} = \begin{Bmatrix} -L \\ M \end{Bmatrix} \quad (1)$$

where h represents the plunge motion and α is the pitch angle. In these equations, x_α is the nondimensional distance between elastic axis and the center of mass, m is the mass of the wing, I_α is the mass moment of inertia of the wing about the elastic axis, b is semichord of wing, c_α, c_h are pitch and plunge structural damping coefficients, k_h is plunge structural spring constant, and L, M are the aerodynamic lift and moment. We assume the quasi-steady aerodynamic forces and moments are modeled as follows [6]:

$$\begin{aligned} L &= \rho U^2 b c_{l_\alpha}\left(\alpha + \frac{\dot{h}}{U} + (\frac{1}{2} - a)b\frac{\dot{\alpha}}{U}\right) + \rho U^2 b c_{l_\beta}\beta \\ M &= \rho U^2 b^2 c_{m_\alpha}\left(\alpha + \frac{\dot{h}}{U} + (\frac{1}{2} - a)b\frac{\dot{\alpha}}{U}\right) + \rho U^2 b^2 c_{m_\beta}\beta \end{aligned} \quad (2)$$

where ρ is the density of air, U is the free stream velocity, $c_{l_\alpha}, c_{m_\alpha}$ are lift and moment coefficients per angle of attack, c_{l_β}, c_{m_β} are lift and moment coefficient per control surface deflection, and a is nondimensional distance from the midchord to the elastic axis. Several classes of nonlinear stiffness contributions $k_\alpha(\alpha)$ have been studied in papers treating the open loop dynamics of aeroelastic systems(see for example, [4, 23, 30, 31]). For purposes of illustration, polynomial nonlinearities are introduced at this point. For example, the polynomial nonlinearities might be expressed as

$$k_\alpha(\alpha) = k_{\alpha_0} + k_{\alpha_1}\alpha + k_{\alpha_2}\alpha^2 + k_{\alpha_3}\alpha^3 + k_{\alpha_4}\alpha^4 + \cdots \quad (3)$$

Combining the two equations (1) and (2), we obtain the equations of motion as

$$\begin{bmatrix} m & mx_\alpha b \\ mx_\alpha b & I_\alpha \end{bmatrix} \begin{Bmatrix} \ddot{h} \\ \ddot{\alpha} \end{Bmatrix} + \begin{bmatrix} c_h + \rho U b c_{l_\alpha} & \rho U b^2 c_{l_\alpha}(\frac{1}{2} - a) \\ \rho U b^2 c_{m_\alpha} & c_\alpha - \rho U b^3 c_{m_\alpha}(\frac{1}{2} - a) \end{bmatrix} \begin{Bmatrix} \dot{h} \\ \dot{\alpha} \end{Bmatrix} + \begin{bmatrix} k_h & \rho U^2 b c_{l_\alpha} \\ 0 & -\rho U^2 b^2 c_{m_\alpha} + k_\alpha(\alpha) \end{bmatrix} \begin{Bmatrix} h \\ \alpha \end{Bmatrix} = \begin{Bmatrix} -\rho b c_{l_\beta} \\ \rho b^2 c_{m_\beta} \end{Bmatrix} U^2\beta \quad (4)$$

For the analysis to follow, it is useful to convert the above equation into a state space formulation. We define the state variable as

$$\mathbf{x} = \begin{Bmatrix} x_1 \\ x_2 \\ x_3 \\ x_4 \end{Bmatrix} = \begin{Bmatrix} h \\ \alpha \\ \dot{h} \\ \dot{\alpha} \end{Bmatrix}$$

The transformed equations of motion become

$$\dot{\mathbf{x}} = \mathbf{f}_\mu(\mathbf{x}) + \mathbf{g}(\mathbf{x})\mu\beta \quad (5)$$

where $\mu = U^2$ and

$$\mathbf{f}_\mu = \begin{Bmatrix} x_3 \\ x_4 \\ -k_1 x_1 - (k_2\mu + p(x_2))x_2 - c_1 x_3 - c_2 x_4 \\ -k_3 x_1 - (k_4\mu + q(x_2))x_2 - c_3 x_3 - c_4 x_4 \end{Bmatrix}, \mathbf{g}(\mathbf{x}) = \begin{Bmatrix} 0 \\ 0 \\ g_3 \\ g_4 \end{Bmatrix}$$

To simplify their form, several auxiliary variables are introduced as shown in Table 1. One should note that the equations of motion are dependent upon the freestream velocity $U(\mu = U^2)$ and also on the elastic axis location a. The notation $\mathbf{f}_\mu(\mathbf{x})$ is conventional in that it emphasizes the parametric dependence of the dynamics on μ and a. Strictly speaking, the subscript μ should be replaced by the vector of the parameters $\{\mu, a\}$. We adopt the simpler notation keeping in mind that the solutions are in fact a two-parameter family of solutions.

3 Open Loop Equations/Limit Cycles

It is well-known that the equations of motion derived above exhibit limit cycle oscillation(LCO), as well as other nonlinear response regimes including chaotic response [20, 4, 31]. The system parameters to be used in following numerical investigations are tabulated in Table 2. These data are obtained from the experimental model of Department of Aerospace Engineering at Texas A&M university. The nonlinear stiffness term $k_\alpha(\alpha)$ is obtained by curve fitting the measured data as [20]

$$k_\alpha(\alpha) = 2.82(1 - 22.1\alpha + 1315.5\alpha^2 - 8580\alpha^3 + 17289.7\alpha^4)$$

With the flow velocity $u = 15(m/s)$ and the initial conditions of $\alpha = 0.1(rad)$ and $y = 0.01(m)$, the resulting time response of the nonlinear system is depicted in Figures 2 and 3. Clearly the system exhibits the limit cycle oscillation and is in good qualitative agreement with the behavior expected in this class of systems. O'Neil, et al.[20, 21, 22] have shown the relations between LCO frequencies, magnitudes and initial conditions or flow velocities. There have been some efforts to control the system using a linear controller[1]. As one might easily expect, however, a linear controller can not effectively stabilize a system which undergoes a severe nonlinear motions and there is a need to design a controller based on nonlinear control methodologies.

4 Feedback Linearization

In this paper, we utilize the method of partial feedback linearization to derive viable control methodologies for the nonlinear aeroelastic system. A detailed description of the feedback linearization methods is beyond the scope of this paper and can be found in various texts, e.g.[11, 19]. Roughly speaking, the method consists of constructing a coordinate transformation which transforms the system equation to a companion form, and selects a nonlinear feedback control law to cancel the nonlinear dynamics. In the most fortunate circumstances, the resulting system is a linear equivalent model, to which modern linear control theory can be easily applied.

However, it is seldom the case that a given nonlinear system is fully linearizable. Depending on the relative degree of the nonlinear system of concern, the nonlinear transformation results in either partially or fully linearized equivalent system. For the case when the system is partially linearized, there exists a hidden internal dynamics whose stability must be investigated to ensure the stability of the whole system [19]. Because it is difficult to find an output function $h(x)$ which yields complete feedback linearization for the two outputs (y, α) in the aeroelastic system with one control surface, we begin by studying two separate problems in which we consider one output variable at a time.

4.1 Pitch Primary Control

In our first study, we will show that the nonlinear equations can be stabilized(at least locally) using partial feedback linearization based on the pitch angle. Since the output and feedback variable are selected to be the pitch angle, we denote this method as "*pitch primary control.*" We begin by calculating the relative degree associated with the following output variable.

$$y = h(\mathbf{x}) = x_2 \tag{6}$$

That is, the objective of the control is to stabilize the pitch output α. The relative degree of the above output is calculated as follows [11]:

$$\begin{aligned} h(\mathbf{x}) &= x_2 \\ L_{\mathbf{f}}h(\mathbf{x}) &= \sum_i \frac{\partial h}{\partial x_i} \cdot f_i = x_4 \\ L_{\mathbf{g}}h(\mathbf{x}) &= \sum_i \frac{\partial h}{\partial x_i} \cdot g_i = 0 \\ L_{\mathbf{g}}L_{\mathbf{f}}h(\mathbf{x}) &= \sum_i \frac{\partial x_4}{\partial x_i} \cdot g_i \\ &= g_4 = \frac{1}{d}(m x_\alpha b^2 \rho c_{l_\beta} + m\rho b^2 c_{m_\beta}) \neq 0 \end{aligned}$$

Thus, we have confirmed that the relative degree of the system is $r = 2$. In other words, 2 degrees of freedom of the system can be linearized. To accomplish partial feedback linearization, we consider the following state transformation

$$\begin{aligned} &\mathbf{x} \mapsto \boldsymbol{\phi} \\ &\phi_1 = h(\mathbf{x}) = x_2 \\ &\phi_2 = L_{\mathbf{f}}h(\mathbf{x}) = x_4 \\ &\phi_3 = x_1 \\ &\phi_4 = -g_3 x_4 + g_4 x_3 \end{aligned} \tag{7}$$

which just happens to be linear. Carefully note that the transform for ϕ_3 and ϕ_4 are defined such that $L_{\mathbf{g}}\phi_3 = 0$ and $L_{\mathbf{g}}\phi_4 = 0$.

To validate that the above transformation is admissible, we need to check the invertibility of the Jacobian of the mapping. The coordinate transformation defined above is

$$\begin{Bmatrix}\phi_1\\ \phi_2\\ \phi_3\\ \phi_4\end{Bmatrix} = \begin{Bmatrix} x_2\\ x_4\\ x_1\\ -g_3x_4 + g_4x_3\end{Bmatrix}, \quad \begin{Bmatrix}x_1\\ x_2\\ x_3\\ x_4\end{Bmatrix} = \begin{Bmatrix} \phi_3\\ \phi_1\\ \frac{1}{g_4}(\phi_4 + g_3\phi_2)\\ \phi_2\end{Bmatrix}$$

The Jacobian matrices of the transform and the inverse transform are

$$\left[\frac{\partial \phi_i}{\partial x_j}\right] = \begin{bmatrix}0 & 1 & 0 & 0\\ 0 & 0 & 0 & 1\\ 1 & 0 & 0 & 0\\ 0 & 0 & g_4 & -g_3\end{bmatrix}, \quad \left[\frac{\partial x_i}{\partial \phi_j}\right] = \begin{bmatrix}0 & 0 & 1 & 0\\ 1 & 0 & 0 & 0\\ 0 & \frac{g_3}{g_4} & 0 & \frac{1}{g_4}\\ 0 & 1 & 0 & 0\end{bmatrix}$$

Since both Jacobians have nonzero determinants, clearly the transform is well-defined. With the above transformation, the governing equations of motion for the system become

$$\begin{Bmatrix}\dot\phi_1\\ \dot\phi_2\\ \dot\phi_3\\ \dot\phi_4\end{Bmatrix} = \begin{Bmatrix} \phi_2\\ -P_\mu(\phi_1)\phi_1 - (c_4 + c_3\frac{g_3}{g_4})\phi_2 - k_3\phi_3 - \frac{c_3}{g_4}\phi_4\\ \frac{g_3}{g_4}\phi_2 + \frac{1}{g_4}\phi_4\\ \begin{pmatrix}\{g_3P_\mu(\phi_1) - g_4Q_\mu(\phi_1)\}\phi_1 +\\ \{-c_1g_3 - c_2g_4 + c_3\frac{g_3^2}{g_4} + c_4g_3\}\phi_2 +\\ +(k_3g_3 - k_1g_4)\phi_3 + \{c_3\frac{g_3}{g_4} - c_1\}\phi_4\end{pmatrix}\end{Bmatrix} + \begin{Bmatrix}0\\ g_4\\ 0\\ 0\end{Bmatrix}\mu\beta \tag{8}$$

where

$$P_\mu(\phi_1) = k_4\mu + q(\phi_1),\ Q_\mu(\phi_1) = k_2\mu + p(\phi_1) \quad (9)$$

Now, partial feedback linearization can be achieved by setting the control input β to be

$$\beta = \frac{P_\mu(\phi_1)\phi_1 + (c_4 + c_3\frac{g_3}{g_4})\phi_2 + k_3\phi_3 + \frac{c_3}{g_4}\phi_4 + v}{\mu g_4} \quad (10)$$

where v is a new, yet to be defined, control. The resulting partially linearized equations are

$$\begin{aligned}
\dot{\phi}_1 &= \phi_2 \\
\dot{\phi}_2 &= v \\
\dot{\phi}_3 &= A_{32}\phi_2 + A_{34}\phi_4 \\
\dot{\phi}_4 &= (g_3 P_\mu(\phi_1) - g_4 Q_\mu(\phi_1))\phi_1 + A_{42}\phi_2 + A_{43}\phi_3 + A_{44}\phi_4
\end{aligned}$$

where,

$$\begin{aligned}
A_{32} &= \frac{g_3}{g_4}, & A_{34} &= \frac{1}{g_4} \\
A_{42} &= -c_1 g_3 - c_2 g_4 + c_3\frac{g_3^2}{g_4} + c_4 g_3 & A_{43} &= k_3 g_3 - k_1 g_4 \\
A_{44} &= \frac{c_3 g_3}{g_4} - c_1
\end{aligned}$$

By judiciously choosing v, we make the linearized dynamics for ϕ_1 and ϕ_2 exponentially stable. We can use any linear control design technique for the linear subsystem $\{\phi_1, \phi_2\}$. However, the subsystem $\{\phi_3, \phi_4\}$ is not affected directly by the new input v and we do not have direct control over this subsystem. Note that the internal dynamics for ϕ_3 and ϕ_4 are still nonlinear. It is generally not easy to investigate the stability of the internal dynamics [19]. However, by checking the stability of the zero dynamics of the partially linearized system, we can obtain stability information on the internal dynamics. Let $\phi_1 = 0$, then clearly $\phi_2 = 0$ and the equation of internal dynamics is

$$\begin{Bmatrix} \dot{\phi}_3 \\ \dot{\phi}_4 \end{Bmatrix} = \begin{bmatrix} 0 & A_{34} \\ A_{43} & A_{44} \end{bmatrix} \begin{Bmatrix} \phi_3 \\ \phi_4 \end{Bmatrix} \quad (11)$$

We observe the zero dynamics is linear and the stability of these zero dynamics will ensure the stability of the entire system, at least locally. The eigenvalues of the zero dynamics are

$$\lambda = \frac{A_{44} \pm \sqrt{A_{44}^2 + 4A_{34}A_{43}}}{2} \quad (12)$$

Note that the stability of the zero dynamics depend on the flow velocity U and on the elastic axis location a, although it is not explicitly shown. With the quantities defined in Table 1, the real parts of the eigenvalues of the zero dynamics are plotted w.r.t. a in Figure 4($U = 15(m/s)$) and in Figure 5($U = 25(m/s)$). Observe that for $a > -0.55$ the real parts of both eigenvalues are negative and thus the zero dynamics is stable. With $a = -0.4, U = 15(m/s)$ and the initial conditions ($\alpha = 0.1(rad), y = 0.01(m)$), the time response of the system is shown in Figure 6. We have chosen the modified input $v = -1.2\dot{\alpha} - 4\alpha$ such that the closed subsystem has poles at $s = -0.6 \pm 1.9079$. It should be emphasized, however, the stability of the zero dynamics only guarantees the local stability of the internal dynamics.

4.2 Plunge Primary Control

In this section we will show that the nonlinear equations can be stabilized(at least locally) using partial feedback linearization in terms of the plunge variable. As in the previous case, we denote this analysis as the "*plunge primary control.*" We begin by investigating the relative degree with the following output variable.

$$y = h(\mathbf{x}) = x_1 \quad (13)$$

That is, the objective of the control is to stabilize the plunge output h. The relative degree of the above output is calculated as follows:

$$\begin{aligned}
h(\mathbf{x}) &= x_1 \\
L_\mathbf{f} h(\mathbf{x}) &= \sum_i \frac{\partial h}{\partial x_i} \cdot f_i = x_3 \\
L_\mathbf{g} h(\mathbf{x}) &= \sum_i \frac{\partial h}{\partial x_i} \cdot g_i = 0 \\
L_\mathbf{g} L_\mathbf{f} h(\mathbf{x}) &= \sum_i \frac{\partial x_4}{\partial x_i} \cdot g_i \\
&= g_3 = \frac{1}{d}(-I_\alpha \rho b c_{l_\beta} - m x_\alpha b^3 \rho c_{m_\beta}) \neq 0
\end{aligned}$$

We have consequently confirmed that the relative degree of the system is $r = 2$. The state transformation we choose for the current case is

$$\begin{aligned}
\mathbf{x} &\mapsto \boldsymbol{\phi} \\
\phi_1 &= h(\mathbf{x}) = x_1 \\
\phi_2 &= L_\mathbf{f} h(\mathbf{x}) = x_3 \\
\phi_3 &= x_2 \\
\phi_4 &= g_3 x_4 - g_4 x_3
\end{aligned} \quad (14)$$

Again, the transform for ϕ_3 and ϕ_4 are defined such that $L_\mathbf{g}\phi_3 = 0$ and $L_\mathbf{g}\phi_4 = 0$. To validate the above

transformation, we need to check that the Jacobian of the transform is nonzero. The coordinate transforms defined above are

$$\begin{Bmatrix}\phi_1\\ \phi_2\\ \phi_3\\ \phi_4\end{Bmatrix}=\begin{Bmatrix}x_1\\ x_3\\ x_2\\ g_3x_4-g_4x_3\end{Bmatrix},\quad \begin{Bmatrix}x_1\\ x_2\\ x_3\\ x_4\end{Bmatrix}=\begin{Bmatrix}\phi_1\\ \phi_3\\ \phi_2\\ \frac{1}{g_3}(\phi_4+g_4\phi_2)\end{Bmatrix}$$

The Jacobian matrices of the transform and inverse transform are

$$\left[\frac{\partial\phi_i}{\partial x_j}\right]=\begin{bmatrix}1&0&0&0\\0&0&1&0\\0&1&0&0\\0&0&-g_4&g_3\end{bmatrix},\quad \left[\frac{\partial x_i}{\partial\phi_j}\right]=\begin{bmatrix}1&0&0&0\\0&0&1&0\\0&1&0&0\\0&\frac{g_4}{g_3}&0&\frac{1}{g_3}\end{bmatrix}$$

Since both Jacobian have nonzero determinants, the transform is well defined, and the governing equations of the system become

$$\begin{Bmatrix}\dot\phi_1\\ \dot\phi_2\\ \dot\phi_3\\ \dot\phi_4\end{Bmatrix}=\begin{Bmatrix}\phi_1\\ -k_1\phi_1-(c_1+c_2\frac{g_4}{g_3})\phi_2-Q_\mu(\phi_3)\phi_3-\frac{c_2}{g_3}\phi_4\\ \frac{g_4}{g_3}\phi_2+\frac{1}{g_3}\phi_4\\ \begin{pmatrix}\{g_4k_1-g_3k_3\}\phi_1\\ +\{c_1g_4+c_2\frac{g_4^2}{g_3}-c_3g_3-c_4g_4\}\phi_2\\ +\{g_4Q_\mu(\phi_3)-g_3P_\mu(\phi_3)\}\phi_3+\{c_2\frac{g_4}{g_3}-c_4\}\phi_4\end{pmatrix}\end{Bmatrix}+\begin{Bmatrix}0\\ g_3\\ 0\\ 0\end{Bmatrix}\mu\beta \quad (15)$$

where

$$P_\mu(\phi_3)=k_4\mu+q(\phi_3),\ Q_\mu(\phi_3)=k_2\mu+p(\phi_3) \quad (16)$$

Clearly, from eq. (15), the feedback linearization can be achieved by setting the control input β to be

$$\beta=\frac{k_1\phi_1+(c_1+c_2\frac{g_4}{g_3})\phi_2+Q_\mu(\phi_3)\phi_3+\frac{c_2}{g_3}\phi_4+v}{\mu g_3} \quad (17)$$

The resulting partially linearized equation is

$$\begin{aligned}\dot\phi_1&=\phi_2\\ \dot\phi_2&=v\\ \dot\phi_3&=A_{32}\phi_2+A_{34}\phi_4\\ \dot\phi_4&=A_{41}\phi_1+A_{42}\phi_2+(g_4Q_\mu(\phi_3)-g_3P_\mu(\phi_3))\phi_3+A_{44}\phi_4\end{aligned}$$

where,

$$A_{32}=\frac{g_4}{g_3},\qquad A_{34}=\frac{1}{g_3}$$

$$A_{41}=g_4k_1-g_3k_3\quad A_{42}=c_1g_4+c_2\frac{g_4^2}{g_3}-c_3g_3-c_4g_4$$

$$A_{44}=c_2\frac{g_4}{g_3}-c_4$$

As in the previous case, since the system is only partially linearized, we are forced to evaluate the stability of the internal dynamics, or, the zero dynamics of the system. By setting $\phi_1=\phi_2=0$, the equation for the zero dynamics is obtained as

$$\begin{Bmatrix}\dot\phi_3\\ \dot\phi_4\end{Bmatrix}=\begin{Bmatrix}A_{34}\phi_4\\ (g_4Q_\mu(\phi_3)-g_3P_\mu(\phi_3))\phi_3+A_{44}\phi_4\end{Bmatrix} \quad (18)$$

Unlike the previous case, the zero dynamics is nonlinear and requires more careful analysis. At a first glance, the zero dynamics (18) has an equilibrium point $(\phi_3,\phi_4)=(0,0)$. However, it turns out that depending on the parameters μ and a, additional equilibrium points exist and we need to perform bifurcation analysis to completely understand the characteristics of the zero dynamics represented by eq. (18). Two sets of bifurcation diagrams are shown in Figures 7 and 8. Figure 7 shows the bifurcation diagram with respect to the flow velocity μ and exhibits the so–called pitch-folk bifurcation [8, 28]. In other words, up to a critical velocity μ_{c_1}, the zero dynamics has only one equilibrium point at $(0,0)$, and is stable. However, beyond μ_{c_1}, there exist two equilibrium points which are stable, whereas the original equilibrium point(origin) is unstable. If the velocity is greater than μ_{c_2} all the equilibrium points are unstable. We observe that the critical velocities μ_{c_1} and μ_{c_2} are dependent on the elastic axis location a and generally, as the elastic axis is moved forward the stable velocity region grows. A typical plot of stable and unstable manifolds are shown in Figure 9. In this case there exist two stable equilibrium points and one unstable equilibrium point. A trajectory will be attracted to either one of the two stable equilibrium points depending on initial conditions. For the case when there are three unstable equilibrium points, the manifolds are plotted in Figure 10. In this case all the trajectories near equilibrium points are divergent. Figure 8 shows the bifurcation diagram with respect to the elastic axis location a. As one might expect the stable region of a is smaller for the greater velocity.

With the initial conditions $y=0.01(m), \alpha=0.1(rad)$ and $a=-0.68, U=15(m/s)$, the time response of the controlled system is shown in Figure 11. We have chosen the modified input $v=-1.2\dot h-4h$ such that the closed subsystem has poles at $s=-0.6\pm 1.9079$. As is expected, the plunge output y and $\dot y$ converges to zero.

5 Feedback Linearization with Two Control Surfaces

In the previous two sections, we have shown that by using a partial feedback linearization method, we can construct locally stable nonlinear controllers for the aeroelastic model. We obtained partially linearized systems and subsequently analyzed the zero dynamics to assure the stability of the closed loop system. However, since the system is only partially linearized, we were only able to obtain local stability results. In this section, we investigate the possibility of obtaining a globally stable nonlinear controller by adding an additional control surface.

By adding another control surface, we assume that the quasi-steady lift and moment of the system is expressed as follows:

$$L = \rho u^2 b c_{l_\alpha}\left(\alpha + \frac{\dot{h}}{U} + (\frac{1}{2}-a)b\frac{\dot{\alpha}}{U}\right) + \rho u^2 b c_{l_{\beta_1}}\beta_1 + \rho u^2 b c_{l_{\beta_2}}\beta_2 \quad (19)$$

$$M = \rho u^2 b^2 c_{m_\alpha}\left(\alpha + \frac{\dot{h}}{U} + (\frac{1}{2}-a)b\frac{\dot{\alpha}}{U}\right) + \rho u^2 b^2 c_{m_{\beta_1}}\beta_1 + \rho u^2 b^2 c_{m_{\beta_2}}\beta_2 \quad (20)$$

The reader is advised that the assumption that the lift and moment can be expressed as simply as depicted in equations (19) and (20) is very restrictive. In particular, it is only appropriate for wing sections that have a very large ratio of span to lateral separation of the control surfaces. As usual, it is likewise limited to small angle of attack, and small control surface displacements. It can be a reasonable representation of lift and moment forces for low speed flow in wind tunnel models with the introduction of a fence or splitter plate as depicted in Figure 12.

Despite the limitations imposed by such a rudimentary aerodynamic model, there are compelling reasons for studying this system from a control theoretic standpoint. We will show in this section that the system depicted in Figure 12 is exactly feedback linearizable provided we know the structural nonlinearities. As such, this analysis provides an approach for designing control systems in which we do not know the exact structure of nonlinearities. The result will be presented without proof at the end of this section.

To begin, we rewrite equation (4)

$$\begin{bmatrix} m & mx_\alpha b \\ mx_\alpha b & I_\alpha \end{bmatrix}\begin{Bmatrix}\ddot{h}\\ \ddot{\alpha}\end{Bmatrix} + \begin{bmatrix} c_h + \rho U b c_{l_\alpha} & \rho U b^2 c_{l_\alpha}(\frac{1}{2}-a) \\ \rho U b^2 c_{m_\alpha} & c_\alpha - \rho U b^3 c_{m_\alpha}(\frac{1}{2}-a)\end{bmatrix}\begin{Bmatrix}\dot{h}\\ \dot{\alpha}\end{Bmatrix} + \begin{bmatrix} k_h & \rho U^2 b c_{l_\alpha} \\ 0 & -\rho U^2 b^2 c_{m_\alpha} + k_\alpha(\alpha)\end{bmatrix}\begin{Bmatrix} h\\ \alpha\end{Bmatrix} = \begin{bmatrix} -\rho b c_{l_{\beta_1}} & -\rho b c_{l_{\beta_2}} \\ \rho b^2 c_{m_{\beta_1}} & \rho b^2 c_{m_{\beta_2}}\end{bmatrix}\begin{Bmatrix}\beta_1\\ \beta_2\end{Bmatrix} U^2 \quad (21)$$

In state space form, the above equation can be compactly written as

$$\dot{\mathbf{x}} = \mathbf{f}_\mu(\mathbf{x}) + \mathbf{g}_1(\mathbf{x})\mu\beta_1 + \mathbf{g}_2(\mathbf{x})\mu\beta_2 \quad (22)$$

where $\mu = u^2$ and

$$\mathbf{f}_\mu = \begin{Bmatrix} x_3 \\ x_4 \\ -k_1 x_1 - (k_2\mu + p(x_2))x_2 - c_1 x_3 - c_2 x_4 \\ -k_3 x_1 - (k_4\mu + q(x_2))x_2 - c_3 x_3 - c_4 x_4 \end{Bmatrix},$$

$$\mathbf{g}_1 = \begin{Bmatrix} 0\\ 0\\ g_{13}\\ g_{14}\end{Bmatrix}, \quad \mathbf{g}_2 = \begin{Bmatrix} 0\\ 0\\ g_{23}\\ g_{24}\end{Bmatrix}$$

Most of the variables in the above equation are defined in Table 1 except g_{ij}'s which are defined as

$$g_{13} = \frac{1}{d}(-I_\alpha \rho b c_{l_{\beta_1}} - m x_\alpha b^3 \rho c_{m_{\beta_1}})$$
$$g_{14} = \frac{1}{d}(m x_\alpha b^2 \rho c_{l_{\beta_1}} + m\rho b^2 c_{m_{\beta_1}})$$
$$g_{23} = \frac{1}{d}(-I_\alpha \rho b c_{l_{\beta_2}} - m x_\alpha b^3 \rho c_{m_{\beta_2}})$$
$$g_{24} = \frac{1}{d}(m x_\alpha b^2 \rho c_{l_{\beta_2}} + m\rho b^2 c_{m_{\beta_2}})$$

Since we have two control surfaces, we consider two output functions such as

$$\mathbf{h}(\mathbf{x}) = \begin{Bmatrix} h_1(\mathbf{x})\\ h_2(\mathbf{x})\end{Bmatrix} = \begin{Bmatrix} x_1\\ x_2\end{Bmatrix} = \begin{Bmatrix} h\\ \alpha\end{Bmatrix} \quad (23)$$

To investigate the relative degree of this multiple degree of freedom system, the following derivatives are needed. For the first output measurement,

$$h_1(\mathbf{x}) = x_1$$
$$L_{\mathbf{f}} h_1(\mathbf{x}) = \sum_i \frac{\partial h_1}{\partial x_i}\cdot f_i = x_3$$
$$L_{\mathbf{g}_1} h_1(\mathbf{x}) = \sum_i \frac{\partial h_1}{\partial x_i}\cdot g_{1i} = 0$$

$$
\begin{aligned}
L_{\mathbf{g}_1}L_{\mathbf{f}}h_1(\mathbf{x}) &= \sum_i \frac{\partial x_3}{\partial x_i}\cdot g_{1i} \\
&= g_{13} = \frac{1}{d}(-I_\alpha \rho b c_{l_{\beta_1}} - m x_\alpha b^3 \rho c_{m_{\beta_1}}) \neq 0 \\
L_{\mathbf{g}_2}h_1(\mathbf{x}) &= \sum_i \frac{\partial h_1}{\partial x_i}\cdot g_{2i} = 0 \\
L_{\mathbf{g}_2}L_{\mathbf{f}}h_1(\mathbf{x}) &= \sum_i \frac{\partial x_3}{\partial x_i}\cdot g_{2i} \\
&= g_{23} = \frac{1}{d}(-I_\alpha \rho b c_{l_{\beta_2}} - m x_\alpha b^3 \rho c_{m_{\beta_2}}) \neq 0
\end{aligned}
$$

For the second output measurement, we require

$$
\begin{aligned}
h_2(\mathbf{x}) &= x_2 \\
L_{\mathbf{f}}h_2(\mathbf{x}) &= \sum_i \frac{\partial h_2}{\partial x_i}\cdot f_i = x_4 \\
L_{\mathbf{g}_1}h_2(\mathbf{x}) &= \sum_i \frac{\partial h_2}{\partial x_i}\cdot g_{1i} = 0 \\
L_{\mathbf{g}_1}L_{\mathbf{f}}h_2(\mathbf{x}) &= \sum_i \frac{\partial x_4}{\partial x_i}\cdot g_{1i} \\
&= g_{14} = \frac{1}{d}(m x_\alpha b^2 \rho c_{l_{\beta_1}} + m\rho b^2 c_{m_{\beta_1}}) \neq 0 \\
L_{\mathbf{g}_2}h_2(\mathbf{x}) &= \sum_i \frac{\partial h_2}{\partial x_i}\cdot g_{2i} = 0 \\
L_{\mathbf{g}_2}L_{\mathbf{f}}h_2(\mathbf{x}) &= \sum_i \frac{\partial x_4}{\partial x_i}\cdot g_{2i} \\
&= g_{24} = \frac{1}{d}(m x_\alpha b^2 \rho c_{l_{\beta_2}} + m\rho b^2 c_{m_{\beta_2}}) \neq 0
\end{aligned}
$$

The following matrix plays a crucial role in defining a linearizing transformation as will be shown shortly.

$$
A(\mathbf{x}) = \begin{bmatrix} L_{\mathbf{g}_1}L_{\mathbf{f}}h_1(\mathbf{x}) & L_{\mathbf{g}_2}L_{\mathbf{f}}h_1(\mathbf{x}) \\ L_{\mathbf{g}_1}L_{\mathbf{f}}h_2(\mathbf{x}) & L_{\mathbf{g}_2}L_{\mathbf{f}}h_2(\mathbf{x}) \end{bmatrix} = \begin{bmatrix} g_{13} & g_{23} \\ g_{14} & g_{24} \end{bmatrix}
$$

Substituting the definitions of g_{ij}, we have

$$
A(\mathbf{x}) = \\
\frac{1}{d}\begin{bmatrix} -I_\alpha \rho b c_{l_{\beta_1}} - m x_\alpha b^3 \rho c_{m_{\beta_1}} & -I_\alpha \rho b c_{l_{\beta_2}} - m x_\alpha b^3 \rho c_{m_{\beta_2}} \\ m x_\alpha b^2 \rho c_{l_{\beta_1}} + m\rho b^2 c_{m_{\beta_1}} & m x_\alpha b^2 \rho c_{l_{\beta_2}} + m\rho b^2 c_{m_{\beta_2}} \end{bmatrix}
$$

The output functions have relative degree of $\{2,2\}$ at $\mathbf{x}_0$ if the matrix $A(\mathbf{x})$ is nonsingular at $\mathbf{x}_0$. The determinant of the matrix $A(\mathbf{x})$ is calculated as:

$$
\begin{aligned}
|A(\mathbf{x})| &= m^2 x_\alpha^2 b^5 \rho^2 (c_{l_{\beta_1}} c_{m_{\beta_2}} - c_{m_{\beta_1}} c_{l_{\beta_2}}) \\
&\quad + m I_\alpha \rho^2 b^3 (c_{m_{\beta_1}} c_{l_{\beta_2}} - c_{l_{\beta_1}} c_{m_{\beta_2}}) \\
&= m\rho^2 b^3 (m x_\alpha^2 b^2 - I_\alpha)(c_{l_{\beta_1}} c_{m_{\beta_2}} - c_{m_{\beta_1}} c_{l_{\beta_2}})
\end{aligned}
$$

Thus unless $m x_\alpha^2 b^2 = I_\alpha$, the nonsingularity of the control influence matrix B guarantees that the system is completely feedback linearizable. The reader should note that this result agrees with our intuition. Suppose, for example, that $c_{l_{\beta_1}} = c_{l_{\beta_2}}$. In this case, the control influence matrix is not invertible, and the results above do not hold. In fact, the wing section control system is equivalent to a single control surface system in this case. Assuming that $A(\mathbf{x})$ is nonsingular, define the state transformation as

$$
\begin{aligned}
\phi_1 &= h_1 = x_1 \\
\phi_2 &= L_{\mathbf{f}}h_1 = x_3 \\
\phi_3 &= h_2 = x_2 \\
\phi_2 &= L_{\mathbf{f}}h_2 = x_4
\end{aligned} \tag{24}
$$

The transformed equation of motion is then

$$
\begin{aligned}
\dot{\phi}_1 &= \phi_2 \\
\dot{\phi}_2 &= L_{\mathbf{f}}^2 h_1 + L_{\mathbf{g}_1}L_{\mathbf{f}}h_1 u_1 + L_{\mathbf{g}_2}L_{\mathbf{f}}h_1 u_2 \\
\dot{\phi}_3 &= \phi_4 \\
\dot{\phi}_4 &= L_{\mathbf{f}}^2 h_1 + L_{\mathbf{g}_1}L_{\mathbf{f}}h_2 u_1 + L_{\mathbf{g}_2}L_{\mathbf{f}}h_2 u_2
\end{aligned} \tag{25}
$$

Observe that

$$
\begin{aligned}
\begin{Bmatrix} \dot{\phi}_2 \\ \dot{\phi}_4 \end{Bmatrix} &= \begin{Bmatrix} L_{\mathbf{f}}^2 h_1 \\ L_{\mathbf{f}}^2 h_1 \end{Bmatrix} + \begin{bmatrix} L_{\mathbf{g}_1}L_{\mathbf{f}}h_1(\mathbf{x}) & L_{\mathbf{g}_2}L_{\mathbf{f}}h_1(\mathbf{x}) \\ L_{\mathbf{g}_1}L_{\mathbf{f}}h_2(\mathbf{x}) & L_{\mathbf{g}_2}L_{\mathbf{f}}h_2(\mathbf{x}) \end{bmatrix} \begin{Bmatrix} \beta_1 \\ \beta_2 \end{Bmatrix} \\
&= \mathbf{b}(\mathbf{x}) + A(\mathbf{x})\boldsymbol{\beta}
\end{aligned}
$$

By choosing

$$
\boldsymbol{\beta} = -A^{-1}(\mathbf{x})(\mathbf{b} + \mathbf{v}) \tag{26}
$$

we obtain completely feedback linearized system:

$$
\begin{aligned}
\dot{\phi}_1 &= \phi_2 \\
\dot{\phi}_2 &= v_1 \\
\dot{\phi}_3 &= \phi_4 \\
\dot{\phi}_4 &= v_2
\end{aligned} \tag{27}
$$

With the same initial conditions as before(i.e., $a = -0.4, U = 15(m/s), \alpha = 0.1(rad), y = 0.01(m)$), the time response of the controlled system is shown in Figure 13. The fictitious input

$$
\mathbf{v} = \begin{Bmatrix} -1.2\dot{h} - 4h \\ -1.2\dot{\alpha} - 4\alpha \end{Bmatrix}
$$

is selected such that the closed linearized system has eigenvalues at $\lambda = \{-0.6 \pm 1.9079, -0.6 \pm 1.9079\}$.

As a final result, we state(without proof) a global stability guarantee for an adaptive control methodology for the two control surface wing, in which we

do not know the structural nonlinearity exactly. For simplicity, we rewrite eq. (21) symbolically as

$$[M]\ddot{\mathbf{x}}+[C_\mu]\dot{\mathbf{x}}+[K_0(\mu)]\mathbf{x}+[W(\mathbf{x})]\mathbf{q}=\mu[B]\begin{Bmatrix}\beta_1\\ \beta_2\end{Bmatrix} \quad (28)$$

where

$$\mathbf{x}=\begin{Bmatrix}h\\ \alpha\end{Bmatrix}, \qquad [K_0(\mu)]=\begin{bmatrix}k_h & \rho U^2 b c_{l_\alpha}\\ 0 & -\rho U^2 b^2 c_{m_\alpha}\end{bmatrix}$$
$$\mathbf{q}=[k_{\alpha_0}\ k_{\alpha_1}\ k_{\alpha_2}\ k_{\alpha_3}\ k_{\alpha_4}]^T$$

and

$$[W(\mathbf{x})]=\begin{Bmatrix}(0\ 0\ 0\ 0\ 0)\\ (\alpha\ \alpha^2\ \alpha^3\ \alpha^4\ \alpha^5)\end{Bmatrix}$$

The reader should carefully note that the nonlinear stiffness terms associated with the pitch angle α have been isolated in the term $[W(\mathbf{x})]\mathbf{q}$. In this section, we assume that the coefficients $\mathbf{q}$ of the polynomial nonlinearity are unknown. The following theorem summarizes the fact that we can derive an adaptive controller for this system that is stable, where estimates $\hat{\mathbf{q}}(t)$ of $\mathbf{q}(t)$ evolve simultaneously with the governing equations (28).

Theorem 5.1. *Suppose we choose the feedback control law*

$$\beta(t)=\frac{1}{\mu}[B]^{-1}\Bigg\{[W(\mathbf{x})]\hat{\mathbf{q}}(t)+\begin{bmatrix}0 & \rho U^2 b c_{l_\alpha}\\ 0 & -\rho U^2 b^2 c_{m_\alpha}\end{bmatrix}\mathbf{x}(t)$$
$$+\begin{bmatrix}\rho U b c_{l_\alpha} & \rho U b^2 c_{l_\alpha}(\frac{1}{2}-a)\\ \rho U b^2 c_{m_\alpha} & -\rho U b^3 c_{m_\alpha}(\frac{1}{2}-a)\end{bmatrix}\dot{\mathbf{x}}(t)-[C_a]\dot{\mathbf{x}}-[K_a]\mathbf{x}\Bigg\}$$

and identification update law

$$\dot{\hat{\mathbf{q}}}(t)=-[\Lambda]^T[W(\mathbf{x})]^T\dot{\mathbf{x}} \quad (29)$$

where $[C_a],[K_a]$ and $[\Lambda]$ are arbitrary symmetric positive definite matrices. Then the trajectories $\mathbf{x}(t),\dot{\mathbf{x}}(t)$ and $\hat{\mathbf{q}}(t)$ are attracted to the largest positive invariant subset of

$$\mathcal{M}=\left\{\begin{Bmatrix}\mathbf{x}\\ \dot{\mathbf{x}}\\ \hat{\mathbf{q}}\end{Bmatrix} : \dot{V}\left(\begin{Bmatrix}\mathbf{x}\\ \dot{\mathbf{x}}\\ \hat{\mathbf{q}}\end{Bmatrix}\right)=0\right\} \quad (30)$$

where

$$V\left(\begin{Bmatrix}\mathbf{x}\\ \dot{\mathbf{x}}\\ \hat{\mathbf{q}}\end{Bmatrix}\right)\equiv\frac{1}{2}\dot{\mathbf{x}}^T[M]\dot{\mathbf{x}}+\frac{1}{2}\mathbf{x}^T\left\{[K_a]+\begin{bmatrix}k_h & 0\\ 0 & 0\end{bmatrix}\right\}\mathbf{x}$$
$$+\frac{1}{2}(\mathbf{q}-\hat{\mathbf{q}})^T[\Lambda]^{-1}(\mathbf{q}-\hat{\mathbf{q}})$$

This result depends, in an intrinsic way, on the results derived in this section. We derive this result in a forthcoming paper.

6 Conclusion

In this paper we have applied a feedback linearization methodology to design nonlinear controllers for a typical wing section with structural nonlinearities. Without any control effort, or with linear controllers, the aeroelastic system reveals various kinds of nonlinear phenomenon including LCO's as noted in various texts[1, 20]. The nonlinear controllers based on the partial feedback linearization yielded a stable closed loop system, although the stability is guaranteed in neighborhood of the equilibrium points. The two crucial parameters – elastic axis location and free stream velocity – have significant effect on the resulting partially linearized closed loop system. In order to derive a globally stabilizing controller, a controller based on two control surfaces has been derived. Under the assumption that the two control surfaces are independent, the nonlinear controller showed exceptional performance in stabilizing the aeroelastic system.

References

[1] Block, J. J. and T. W. Strganac, "Applied Active Control for a Nonlinear Aeroelastic Structure," *Journal of Guidance, Control, and Dynamics*, in review, June 1996.

[2] Breitbach, E. J., *Effects of Structural Nonlinearities on Aircraft Vibration and Flutter*, AGARD-R-665, Jan 1978, North Atlantic Treaty Organization, Neuilly sur Seine, France.

[3] Dowell, E. H. and M. Ilgamov, *Studies in Nonlinear Aeroelasticity*, Springer-Verlag, New York, 1988.

[4] Dowell, E. H, "Nonlinear Aeroelasticity," *Proceedings of the AIAA 31st Structures, Structural Dynamics, and Materials Conference*, AIAA, pp. 1497-1509, 1990.

[5] Edwards, J. W. , H. Ashley, and J. Breakwell, J., "Unsteady Aerodynamic Modeling for Arbitrary Motions," *AIAA Journal*, Vol. 17, No. 4, April 1979, pp. 365-374. 1996.

[6] Fung, Y. C., *An Introduction to the Theory of Aeroelasticity*, John Wiley & Sons, New York, 1955.

[7] Gangsaas, D., U. Ly, and D. C. Norman, "Practical Gust Load Alleviation and Flutter Suppression Control Laws Based on LQG Methodology," *Proceedings of the 19th Aerospace Sciences Meeting*, American Institute of Aeronautics and Astronautics, AIAA Paper No. 81-0021, Jan. 1981, pp 1-10.

[8] Guckenheimer, J. and P. Holmes, *Nonlinear Oscillations, Dynamical Systems, and Bifurcations of Vector Fields*, Springer–Verlag, New York, 1983.

[9] Heeg, J., Analytical and Experimental Investigation of Flutter Suppression by Piezoelectric Actuation, *NASA Technical Paper 3241*, 1993, National Aeronautics and Space Administration.

[10] Horikawa, H. and E. H. Dowell, "An Elementary Explanation of the Flutter Mechanism with Active Feedback Controls," *Journal of Aircraft*, Vol. 16, No. 4, Apr. 1979, pp. 225-232.

[11] Isidori, A., *Nonlinear Control Systems*, Springer-Verlag, New York, 1989.

[12] Karpel, M., "Design for Active Flutter Suppression and Gust Alleviation Using State-Space Aeroelastic Modeling," *Journal of Aircraft*, Vol. 19, No. 3, Mar. 1982, pp. 221-227.

[13] Lazarus, K., Multivariable High-Authority Control of Plate-Like Active Lifting Surfaces, *Ph.D. Dissertation*, June 1992, Massachusetts Institute of Technology.

[14] Lazaraus, K., E. Crawley, and C. Lin, "Fundamental Mechanisms of Aeroelastic Control with Control Surface and Strain Actuation," *Journal of Guidance, Control, and Dynamics*, Vol. 18, No. 1, Jan. 1995, pp. 10-17.

[15] Lee, B. H. K., and P. LeBlanc, Flutter Analysis of a Two-Dimensional Airfoil with Cubic Nonlinear Restoring Force, National Aeronautical Establishment, Aeronautical Note - 36, National Research Council (Canada) No. 25438, Ottawa, Quebec, Canada, Feb. 1986.

[16] Lin, C. Y., Strain Actuated Aeroelastic Control, *M. S. Thesis*, Feb. 1993, Massachusetts Institute of Technology.

[17] Lyons, M. G., R. Vepa, S. C. McIntosh, and D. B. DeBra, "Control Law Synthesis and Sensor Design for Active Flutter Suppression," *Proceedings of the AIAA Guidance and Control Conference*, American Institute of Aeronautics and Astronautics, AIAA Paper No. 73-832, 1973, pp. 1-29.

[18] Mukhopadhyay, V., J. R. Newsom, and I. Abel, "A Direct Method for Synthesizing Low-Order Optimal Feedback Control Laws With Application to Flutter Suppression," *Proceedings of the Atmospheric Flight Mechanics Conference*, American Institute of Aeronautics and Astronautics, AIAA Paper No. 80-1613, Aug. 1980, pp 465-475.

[19] Slotine, J. E. and W. Li, *Applied Nonlinear Control*,Prentice-Hall, New Jersey, 1991.

[20] O'Neil, T. and T. W. Strganac, "An Experimental Investigation of Nonlinear Aeroelastic Respons," *AIAA Journal of Aircraft*, accepted for publication, October 1995.

[21] O'Neil T. and T. W. Strganac, "Nonlinear Aeroelastic Response – Analyses and Experiments," *Proceedings of the AIAA 34th Aerospace Sciences Meeting & Exhibit*, AIAA Paper No. 96-0014, 1996.

[22] O'Neil, T., H. C. Gilliatt, and T. W. Strganac, "Investigations of Aeroelastic Response for a System with Continuous Structural Nonlinearitie," AIAA Paper 96-1390, *37th AIAA Structures, Structural Dynamics, and Materials Conference*, Salt Lake City, Utah, April 1996.

[23] Tang, D. M. and E. H. Dowell, "Flutter and Stall Response of a Helicopter Blade with Structural Nonlinearity," *Journal of Aircraft*, Vol. 29, pp. 953-960, 1990.

[24] Theodorsen, T., *General Theory of Aerodynamic Instability and the Mechanism of Flutter*, NACA Report 496, National Advisory Committee for Aeronautics, Hampton, Virginia, 1935.

[25] Theodorsen, T., and I. E. Garrick, *Mechanism of Flutter: A Theoretical and Experimental Investigation of the Flutter Problem*, NACA Report 685, National Advisory Committee for Aeronautics, Hampton, Virginia, 1940.

[26] Vepa, R., The Use of Pade Approximants to Represent Unsteady "Aerodynamic Loads for Arbitrary Small Motions of Wings," *American Institute of Aeronautics and Astronautics*, AIAA Paper No. 76-17, 1976.

[27] Wagner, H. and R. T. Jones, see [6].

Table 1: System Variables

$d = m(I_\alpha - mx_\alpha^2 b^2)$	
$k_1 = \frac{I_\alpha k_h}{d}$	$k_2 = \frac{I_\alpha \rho b c_{l_\alpha} + m x_\alpha b^3 \rho c_{m_\alpha}}{d}$
$k_3 = \frac{-m x_\alpha b k_h}{d}$	$k_4 = \frac{-m x_\alpha b^2 \rho c_{l_\alpha} - m\rho b^2 c_{m_\alpha}}{d}$
$p(x_2) = \frac{-m x_\alpha b}{d} k_\alpha(x_2)$	$q(x_2) = \frac{m}{d} k_\alpha(x_2)$
$c_1 = \frac{I_\alpha (c_h + \rho U b c_{l_\alpha}) + m x_\alpha \rho U b^3 c_{m_\alpha}}{d}$	$c_2 = \frac{I_\alpha \rho U b^2 c_{l_\alpha}(\frac{1}{2}-a) - m x_\alpha b c_\alpha + m x_\alpha \rho U b^4 c_{m_\alpha}(\frac{1}{2}-a)}{d}$
$c_3 = \frac{-m x_\alpha b c_h - m x_\alpha \rho U b^2 c_{l_\alpha} - m\rho U b^2 c_{m_\alpha}}{d}$	$c_4 = \frac{m c_\alpha - m x_\alpha \rho U b^3 c_{l_\alpha}(\frac{1}{2}-a) - m\rho U b^3 c_{m_\alpha}(\frac{1}{2}-a)}{d}$
$g_3 = \frac{1}{d}(-I_\alpha \rho b c_{l_\beta} - m x_\alpha b^3 \rho c_{m_\beta})$	$g_4 = \frac{1}{d}(m x_\alpha b^2 \rho c_{l_\beta} + m\rho b^2 c_{m_\beta})$

Table 2: System Parameters

b	$0.135m$	ρ	$1.225kg/m^3$
span	$0.6m$	c_{l_α}	6.28
k_h	$2844.4N/m$	c_{l_β}	3.358
c_h	$27.43Ns/m$	c_{m_α}	$(0.5+a)c_{l_\alpha}$
		c_{m_β}	-0.635

[28] Wiggins, S., *Introduction to Applied Nonlinear Dynamical Systems, and Chaos*,Springer–Verlag, New York, 1990.

[29] Woolston, D. S., H. L. Runyan, and R. E. Andrews, "An Investigation of Effects of Certain Types of Structural Nonlinearities on Wing and Control Surface Flutter," *Journal of Aeronautical Sciences*, Vol. 24, No. 1, Jan. 1957, pp. 57-63.

[30] Yang, Z. C. and L. C. Zhao, "Analysis of Limit Cycle Flutter of an Airfoil in Incompressible Flow," *Journal of Sound and Vibration*, Vol. 123, No. 1, pp. 1–13, 1988.

[31] Zhao, L. C. and Z. C. Yang, "Chaotic Motions of an Airfoil with Nonlinear Stiffness in Incompressible Flow," *Journal of Sound and Vibration*, Vol. 138, No. 2, pp. 245–254. 1990.

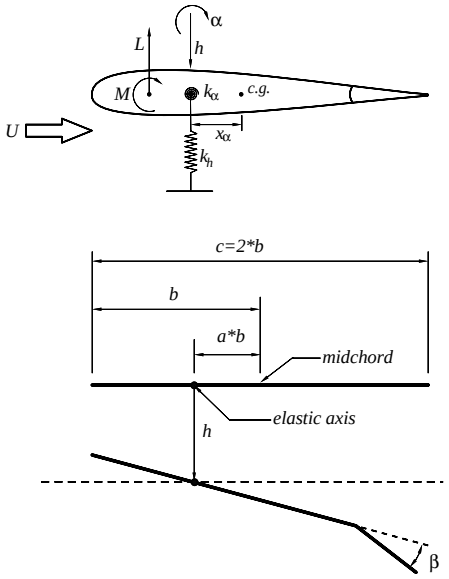

Figure 1: Aeroelastic Model

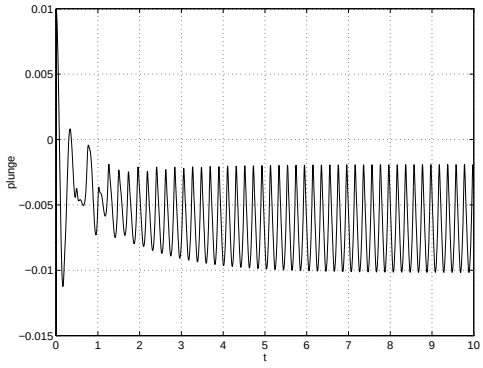

Figure 2: Open Loop Response : Plunge

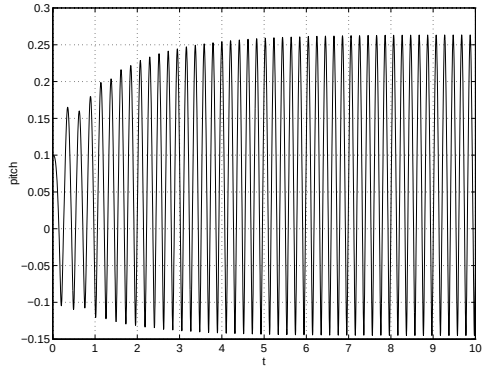

Figure 3: Open Loop Response : Pitch

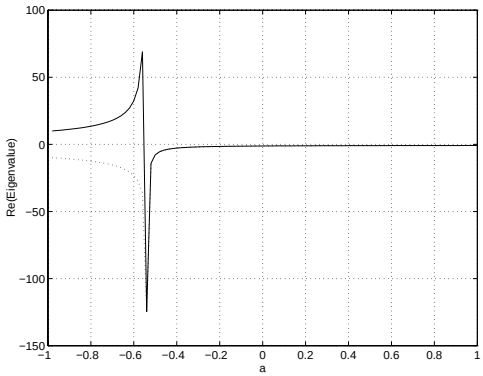

Figure 4: Real Parts of Eigenvalues of Zero Dynamics w.r.t. a (pitch primary, $U = 15(m/s)$)

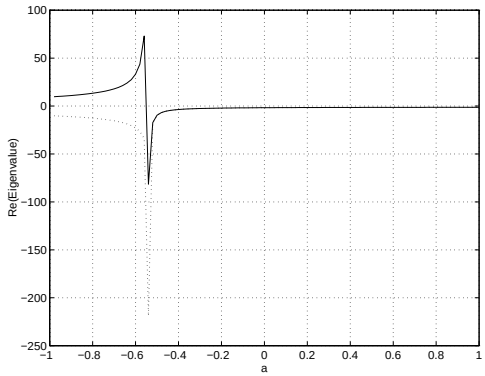

Figure 5: Real Parts of Eigenvalues of Zero Dynamics w.r.t. a (pitch primary, $U = 25(m/s)$)

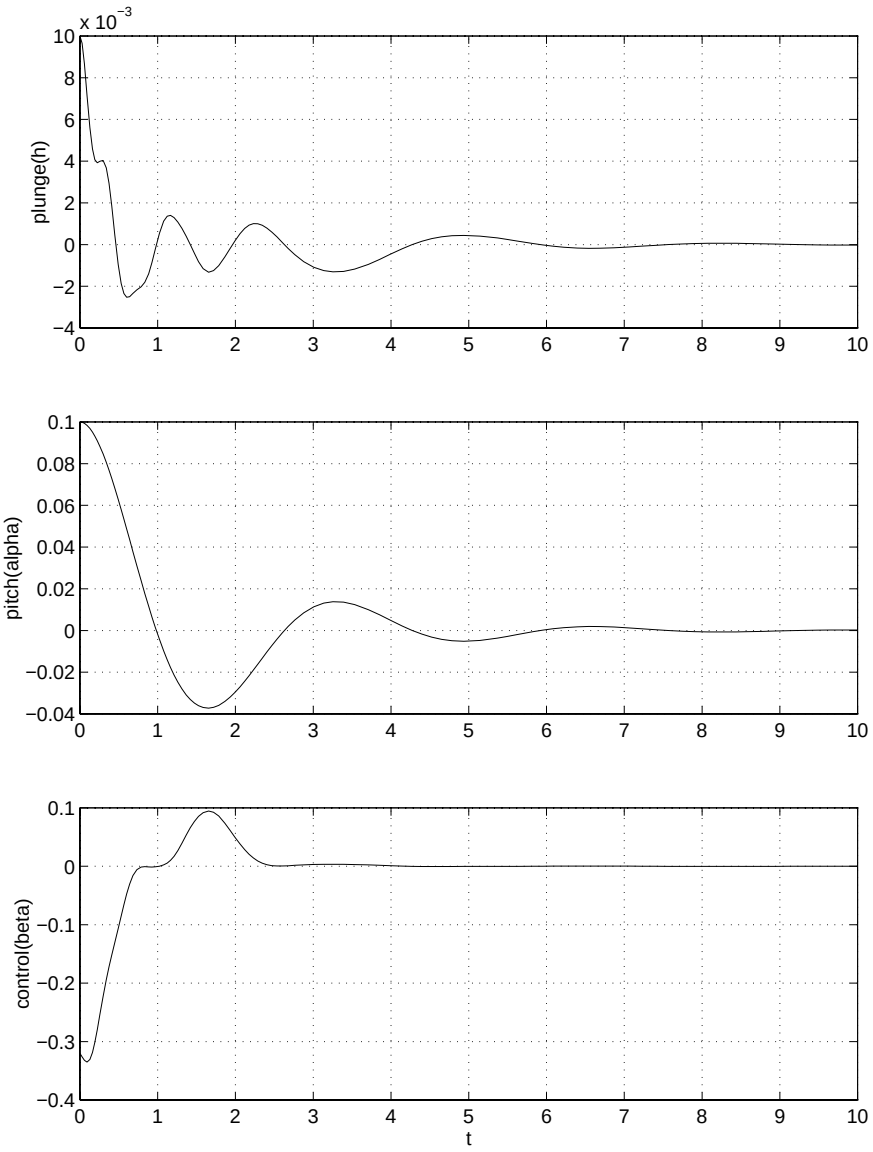

Figure 6: Time Response of Pitch Primary Control($a = -0.4, U = 15(m/s)$)

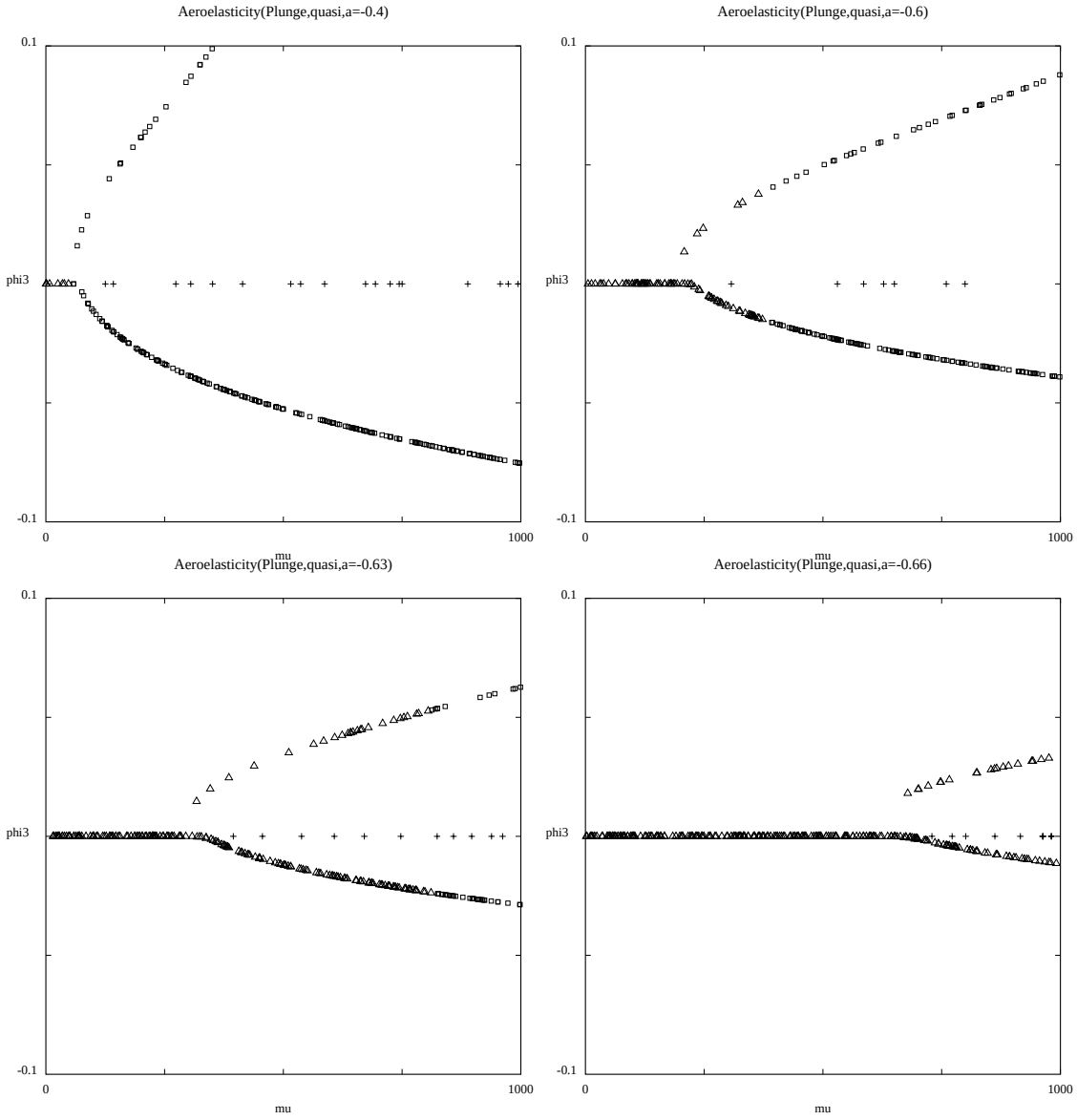

Figure 7: Bifurcation Diagrams for Zero Dynamics for Plunge Primary Control(w.r.t. μ)

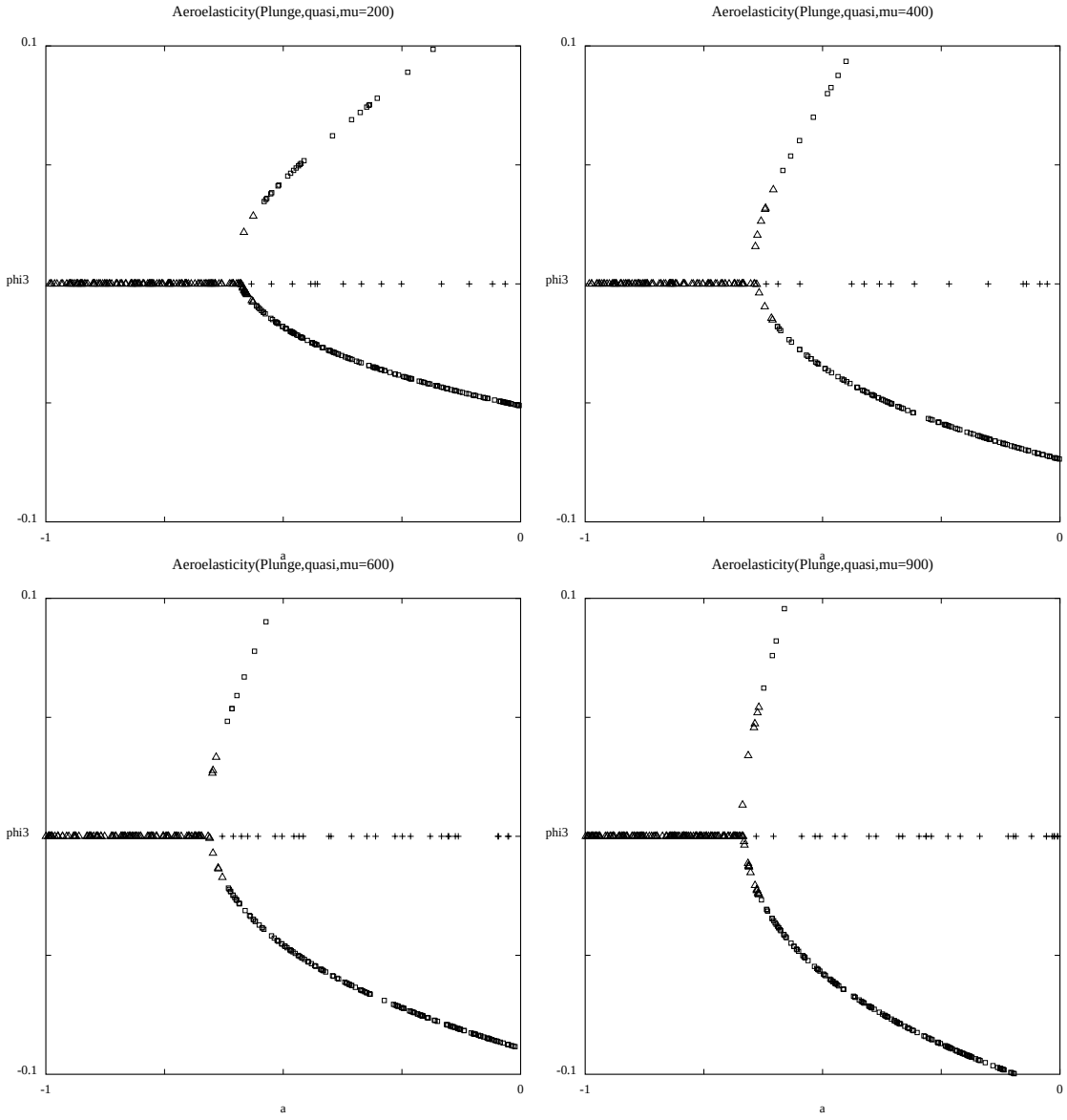

Figure 8: Bifurcation Diagrams for Zero Dynamics for Plunge Primary Control(w.r.t. a)

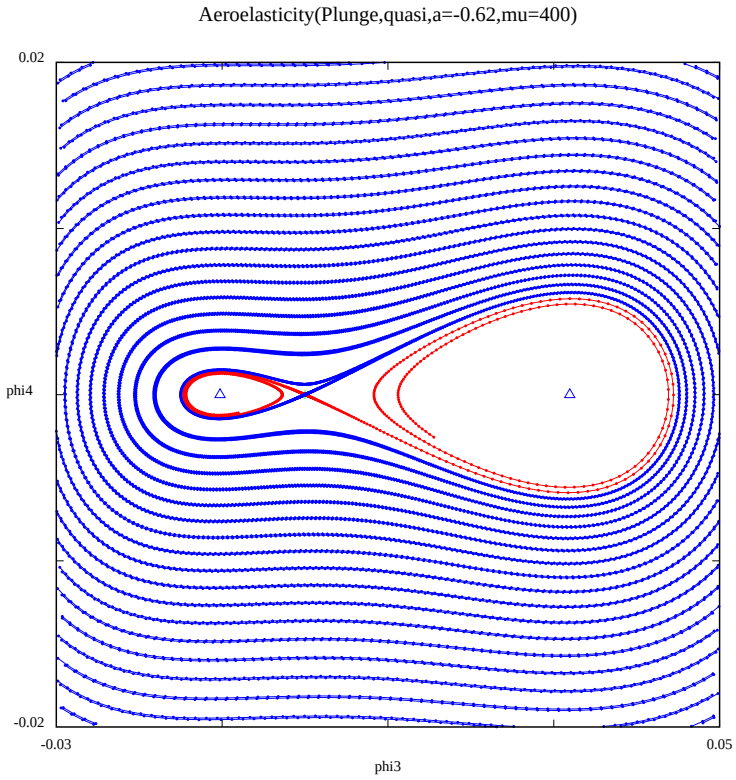

Figure 9: Stable and Unstable Manifolds of Equilibrium Point $(0, 0)$ for Two Stable and One Unstable Equilibrium Case

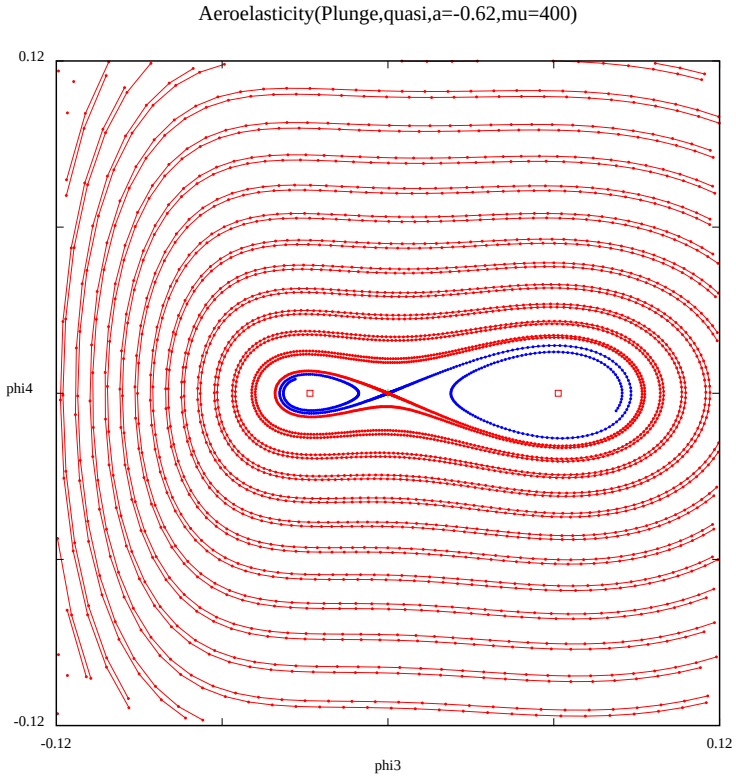

Figure 10: Stable and Unstable Manifolds of Equilibrium Point $(0, 0)$ for Three Unstable Equlibrium Case

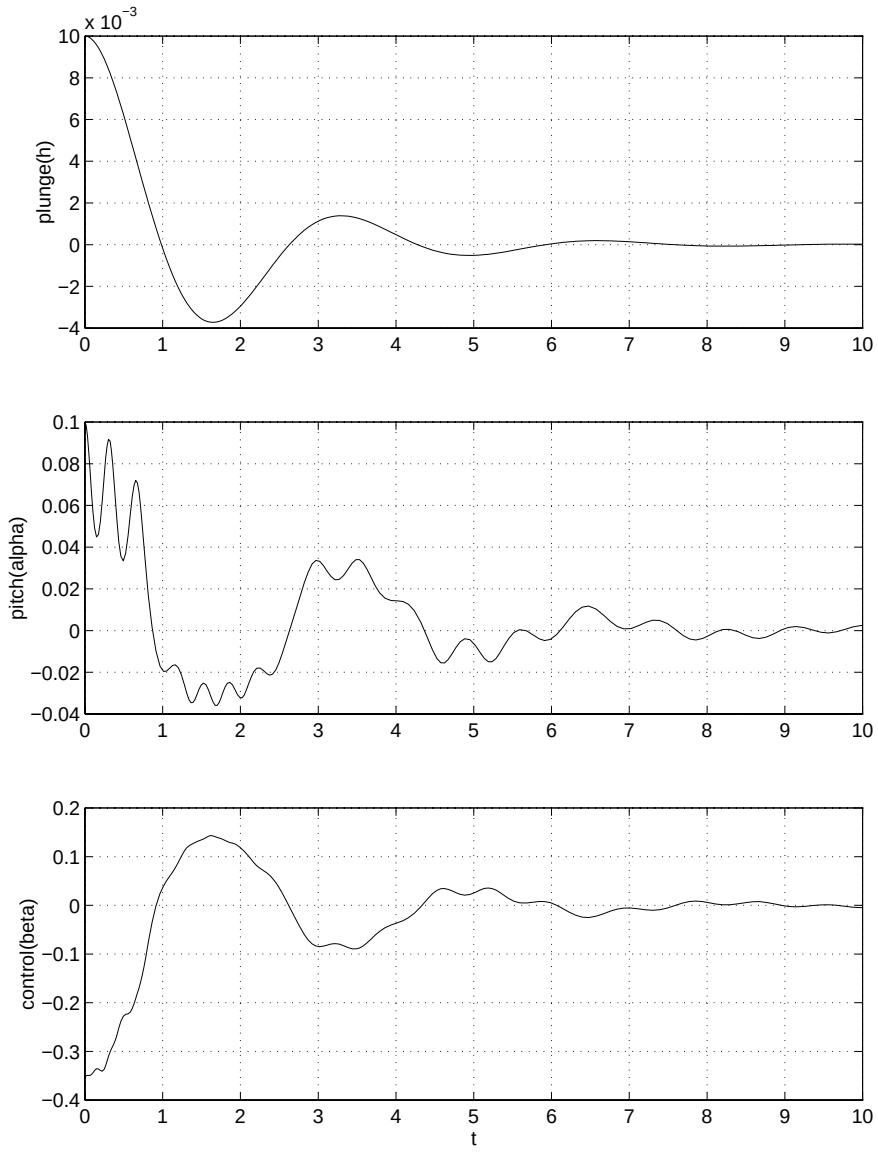

Figure 11: Time Response of Plunge Primary Control($a = -0.68, U = 15(m/s)$)

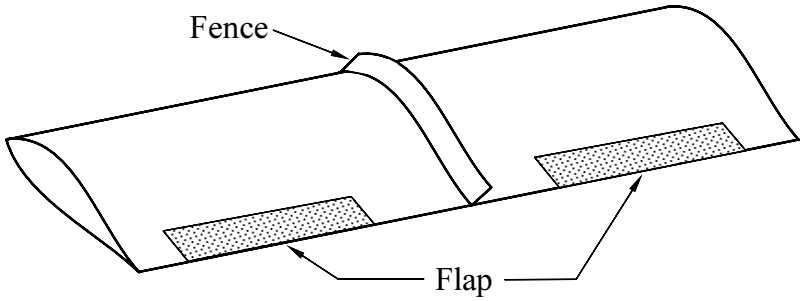

Figure 12: Wing with Two control Surfaces

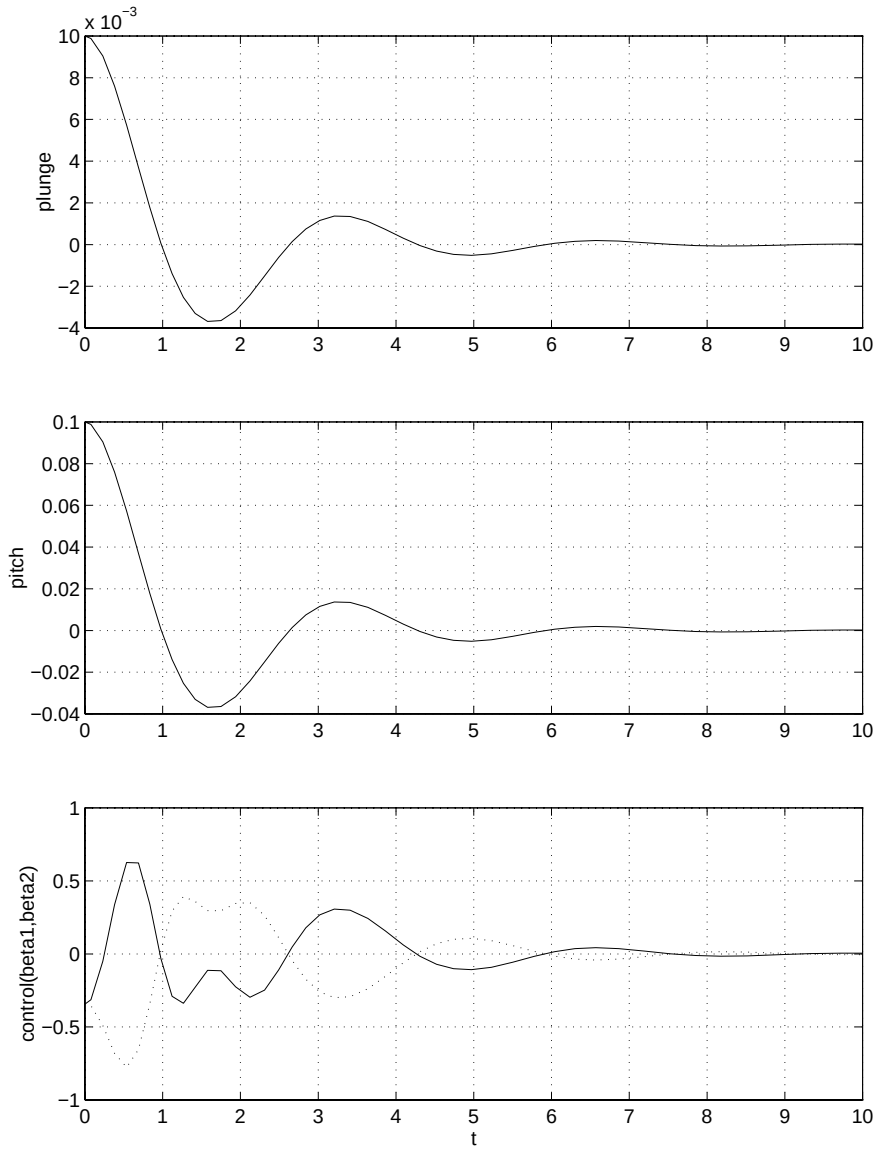

Figure 13: Time Response with Two Control Surfaces ($a = -0.4, U = 15(m/s)$)